(20) Ungar, G.; Organ, S. J.; Keller, A. J. Polym. Sci., Polym. Lett. Ed. 1988, 26, 259.
(21) Following completion of the present paper we have learned in private communication from Professor D. C. Bassett that he and his collaborators have also observed asymmetrical lateral growth of one lamella growing upon another as substrate (in their case at screw dislocations exposed by permanganic acid etching of bulk samples of polyethylene).

Melting and Crystallization of Gelation Crystallized Ultrahigh Molecular Weight Polyethylene

Thein Kyu,* Kenichi Fujita, Myung H. Cho, and Takeshi Kikutani

Center for Polymer Engineering, University of Akron, Akron, Ohio 44325

Jar-Shyong Lin

National Center for Small-Angle Scattering Research, Solid-State Division, Oak Ridge National Laboratory, Oak Ridge, Tennessee 37831. *Received June 3, 1988; Revised Manuscript Received October 26, 1988*

ABSTRACT: Melting and crystallization phenomena of gelation crystallized ultrahigh molecular weight polyethylene (UHMWPE) were studied by means of small-angle X-ray scattering (SAXS), wide-angle X-ray diffraction (WAXD), and small-angle light scattering (SALS). The initial morphology of the gelation crystallized UHMWPE is similar to stacked single crystal mats with preferential c-axis orientation normal to the film surface. Annealing below T_m has resulted in a drastic increase of SAXS long period which has been customarily attributed to lamellar thickening. However, WAXD studies show a remarkable reduction of crystallinity during annealing, indicative of melting and recrystallization rather than lamellar thickening. When the temperature increases beyond T_m, the WAXD crystalline peaks disappear, but a slight amorphous orientation persists in the melt state. SALS and SAXS scattering also occur in the melt, suggesting the presence of melt anisotropy of UHMWPE associated with the slow diffusion of extremely long chains. Upon cooling from the melt (200 °C), well-grown truncated spherulites developed with the appearance of concentric fringes characteristic of lamellar twisting. The average diameter of these spherulites is 100 μm with a twist period of 2–3 μm.

Introduction

Gel processing of ultrahigh molecular weight polyethylene (UHMWPE), such as gel extrusion, spinning, and drawing, has been the subject of recent interest for its potential in applications such as high strength and high modulus fibers.[1-5] It is therefore natural that most studies have been focused on the establishment of the relationship between structure and properties of gel processed UHMWPE.[6-11] Little attention has been paid to the melt behavior of the materials because conventional melt processing methods are not applicable due to the very high melt viscosity associated with extremely high molecular weight.

A number of studies report on the peculiar melt behavior of UHMWPE. Pennings and co-workers[8,9] observed the presence of superheated crystals in the melt (190 °C) of the solution-grown shish-kebab structure, showing the change of orthorhombic to hexagonal structure as a result of the crystal a-axis expansion. The transformation of the orthorhombic to the hexagonal rotator phase was observed by Matsuo and Sawatari[10] in a cross-linked UHMWPE melt, who showed that the hexagonal phase was stable up to 230 °C. The authors concluded that such ordered melt is associated with the strong superheating behavior of cross-linked UHMWPE.

We are intrigued by the observation of Zachariades and Logan,[12] who observed the birefringent UHMWPE melt above the crystal melting temperature. The authors noted that the melt anisotropy of UHMWPE cannot be accounted for solely by the superheating of the crystalline phase or orientation effects in the melt. Instead, they suggested that an ordered region, reminiscent of smectic liquid crystals having orthorhombic (type E) or hexagonal (type B) structure, might exist in the melt.

Recently, the melt behavior of UHMWPE was studied by Wunder and Merajver[13] using Raman spectroscopy in the temperature range of 135–208 °C, a region where the melt anisotropy was observed. The authors confirmed the presence of ordered regions in the UHMWPE melt in which part of the polyethylene chain is in an environment that is similar to that of the orthorhombic polyethylene crystal. They concluded that the melt anisotropy of UHMWPE arises primarily from slowly melting superheated oriented crystals but not from a smectic liquid crystalline phase.

It is felt that further investigation on the structure of ordered UHMWPE melt is needed to reconcile the different opinions. In this paper the melting and crystallization of gelation crystallized UHMWPE has been examined by using small-angle X-ray scattering (SAXS), wide-angle X-ray diffraction (WAXD), small-angle light scattering (SALS), and optical microscopic methods. We address three issues: (1) the lamellar thickening or melting and recrystallization during annealing below T_m, (2) the melt structure above T_m, and (3) the formation of large spherulites during recrystallization from the UHMWPE melt.

Experimental Section

UHMWPE ($M_w \sim 6 \times 10^6$, Himont Co.) was dissolved in Decalin by rigorously stirring at 155 °C for 30 min in a nitrogen environment to prevent oxidation of the specimens. The polymer concentration was 0.4% (w/v) and Irgonox-1076 (Ciba-Geigy Co.) was added as antioxidant (0.1% w/w on polymer). The hot solution was quickly transferred to a stainless-steel tray and slowly cooled under quiescent conditions to form gels. Decalin solvent oozed out during gelation crystallization and was removed gradually by siphoning. During gelation crystallization, the gels were slightly pressed between glass plates to improve the uniformity and surface smoothness of the film. The residual Decalin

* To whom correspondence should be addressed.

0024-9297/89/2222-2238$01.50/0

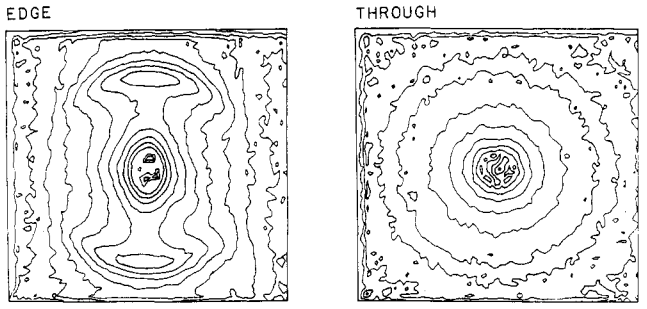

Figure 1. Two-dimensional SAXS isointensity contour patterns for the edge and through view of the gelation crystallized UHMWPE.

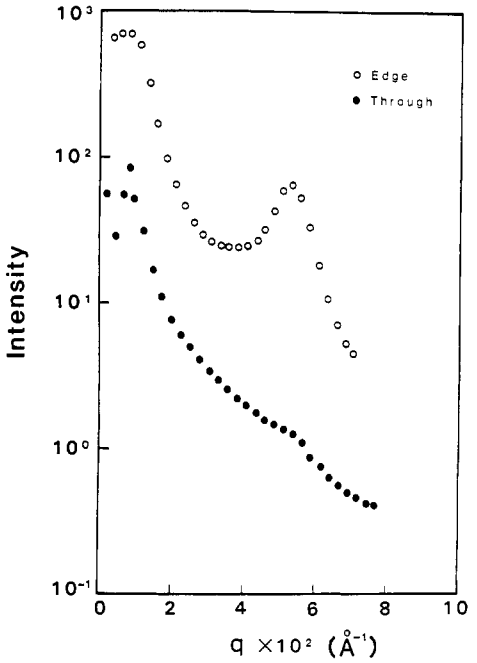

Figure 2. Comparison of SAXS intensity versus scattering wavenumber (q) curves for the edge and through views.

was removed by slowly evaporating it in a fume hood at room temperature for about 3 weeks, then the films were further dried at 70 °C for a minimum of 72 h. For light-scattering studies, the thickness of the films was adjusted to about 10 μm, but thicker films (300 μm) were prepared for X-ray studies.

SAXS isointensity contours were obtained on the ORNL (Oak Ridge National Laboratory) 10-m SAXS camera with a 20 cm × 20 cm two-dimensional position-sensitive detector. WAXD pictures and intensity profiles were acquired by using a 12 kW Rigaku X-ray generator. Polarized optical micrographs were taken on a Leitz microscope (Laborlux 12) at 400× magnification. SALS pictures were photographed by using a Polariod camera (Land film holder 545) with a set of polarizers. A He–Ne laser with a wavelength of 632.8 nm was utilized as a light source. Differential scanning calorimetry experiments were undertaken under nitrogen blanket in a Du Pont 9900 thermal analyzer. An indium standard was utilized for temperature calibration. The heating rate of 10 °C/min was chosen arbitrarily.

Results

Small-angle X-ray scans of gelation crystallized UHMWPE films were acquired from through view (normal to the film surface) and edge view by using the 10-m SAXS facility at Oak Ridge National Laboratory. As can be witnessed in Figure 1, there are appreciable differences in the scattering patterns in through and edge views. The isointensity contour in the through view appears isotropic without showing a definitive maximum, whereas in the edge view, it shows a two-point pattern. Figure 2 shows a plot of SAXS intensity against scattering wavenumber,

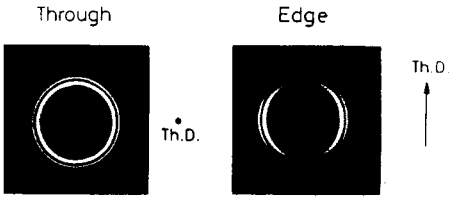

Figure 3. WAXD patterns of gelation crystallized UHMWPE: (a) in the through view and (b) in the edge view.

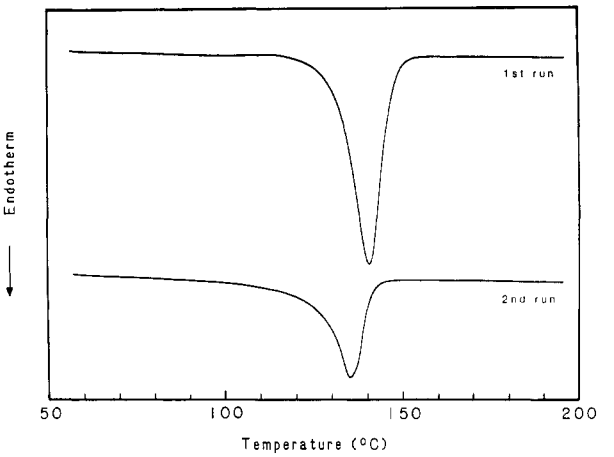

Figure 4. DSC thermograms of gelation crystallized UHMWPE: (a) the first run of the original gelation crystallized film and (b) the second run, after cooling from the melt.

$q = (4\pi/\lambda) \sin \theta$, where 2θ is the scattering angle and λ the wavelength of the X-rays. A distinct SAXS maximum develops in the edge view, whereas a small shoulder peak is discerned in the through view. The scattered intensity in the former is 1 order of magnitude greater than in the latter case. It should be pointed out that this small peak in the through view is completely absent if there was no external disturbance during gelation crystallization. The peak becomes more pronounced if the gels were pressed during gelation crystallization. The long period as estimated from those SAXS peaks is about 118 Å.

As can be seen in Figure 3, wide-angle X-ray diffraction (WAXD) patterns in the through view are isotropic, while in the edge view, the (110) and (200) arcs appear in the equatorial direction, indicating the preferential c-axis orientation normal to the film surface. The WAXD results combined with the above SAXS observation strongly suggest that the structure of the gelation crystallized film is reminiscent of single-crystal mats, which is in good agreement with the results reported by Matsuo and Manley.[7]

DSC thermograms were obtained for the gelation crystallized UHMWPE films and depicted in Figure 4. The crystal melting endothermic peak is located around 142 °C. However in the second run, after cooling from the melt, the T_m shifts to 135 °C. The melting peak remains fairly constant in the subsequent runs. The heat of fusion reduces appreciably, implying that the degree of crystallinity must decrease during recrystallization from the melt. Assuming the heat capacity of the pure PE crystals to be 68.4 cal/g,[14] the crystallinity was estimated to be 84% in the initial gelation crystallized UHMWPE, but it reduced to 50% when the samples recrystallized from the melt.

In Figures 5 and 6 are shown the changes of SAXS patterns during the course of heating in the through and edge views, respectively. The circular pattern of the through view shows little or no changes in its shape. However, the maximum peak of the two-point pattern in the edge view shifts to the center. The shape of the

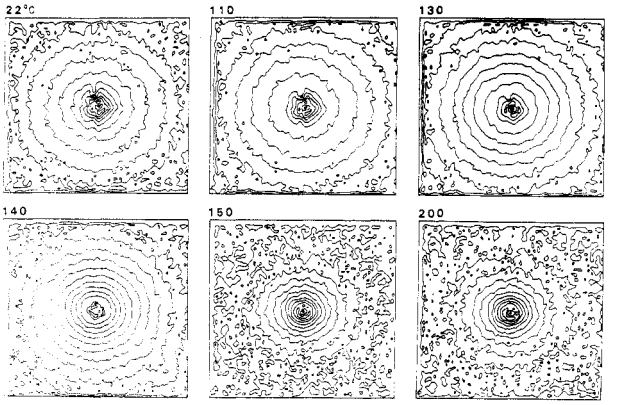

Figure 5. Variation of SAXS patterns during the course of heating in the through view.

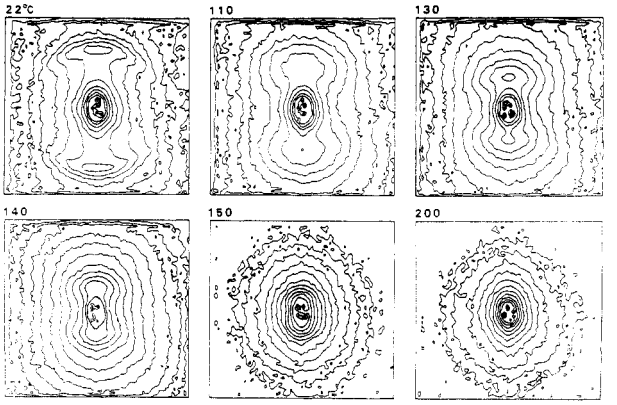

Figure 6. Variation of SAXS patterns during the course of heating in the edge view.

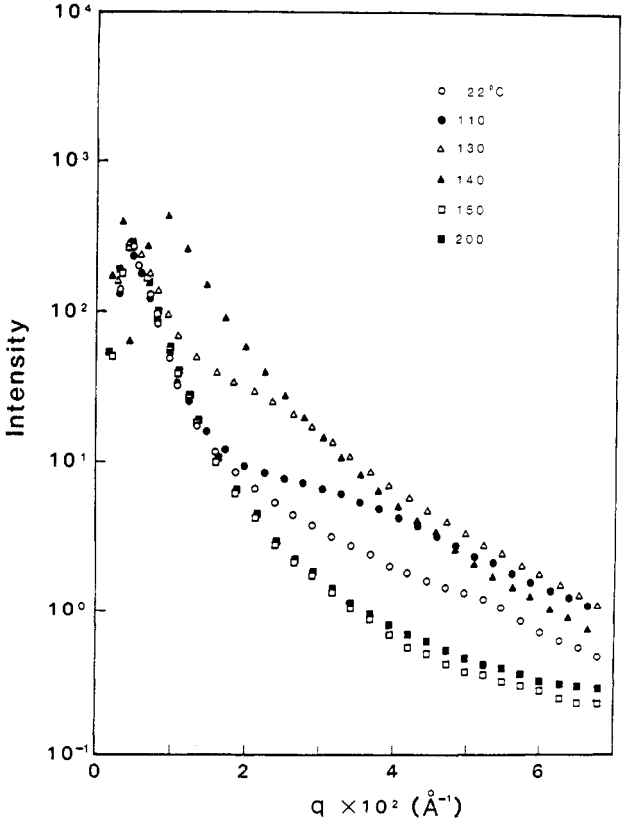

Figure 7. Change of SAXS intensity as a function of wavenumber in the through view.

two-point contour changes appreciably to an elliptical shape with continued heating beyond the crystal melting temperature. It is interesting to note that the weakly

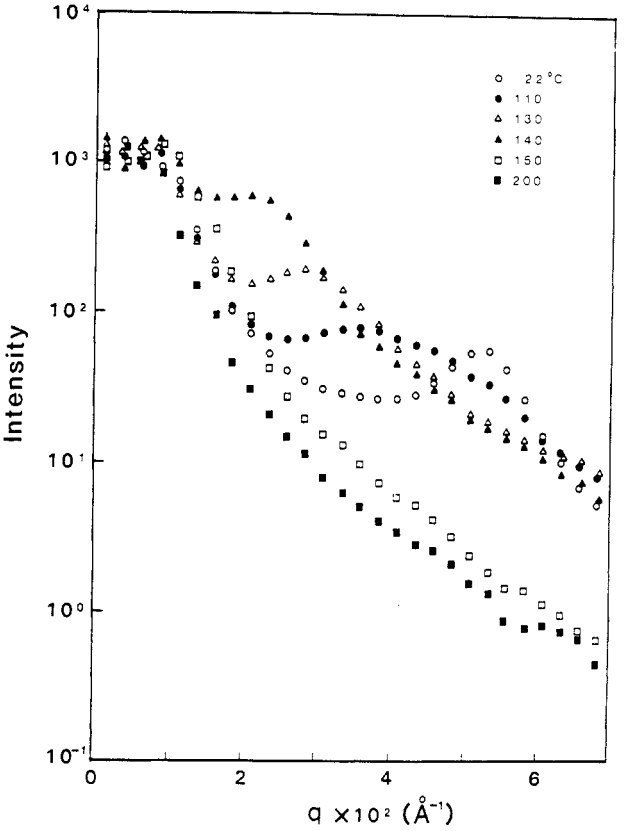

Figure 8. Change of SAXS intensity as a function of wavenumber in the edge view.

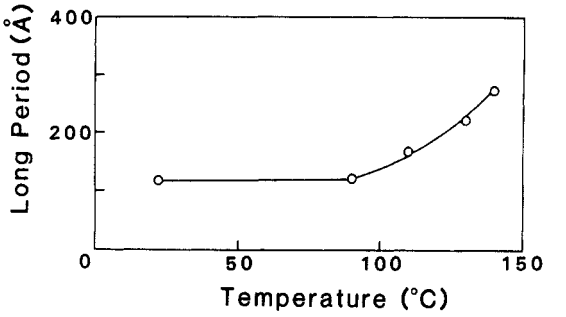

Figure 9. Change of long period as a function of annealing temperature.

anisotropic SAXS pattern persists above the crystal melting temperature, suggesting that some kind of ordered structure might be present in the UHMWPE melt. This aspect will be discussed later in conjunction with the WAXD results.

The variation of the scattered intensity is further analyzed in Figures 7 and 8. Since the SAXS peak in the through view is initially very small, the change of intensity curves is rather subtle. This scenario is more prominent in the case of edge view in which the peak intensity increases immensely while its position moves to lower scattering angles, reflecting an increase in the long period. Figure 9 illustrates the change of long period as a function of temperature. The long period was measured within 5 min after the said temperature had been reached. The increase in long period has been customarily attributed to the lamellar thickening.[15,16]

However, the WAXD results in the through view of Figure 10a show an appreciable decrease of (110) and (200) peak intensities during annealing, while the amorphous scattering increases. This trend has also been observed in the edge view in Figure 10b, but to a lesser extent. Since the structure in the edge view is anisotropic, the WAXD

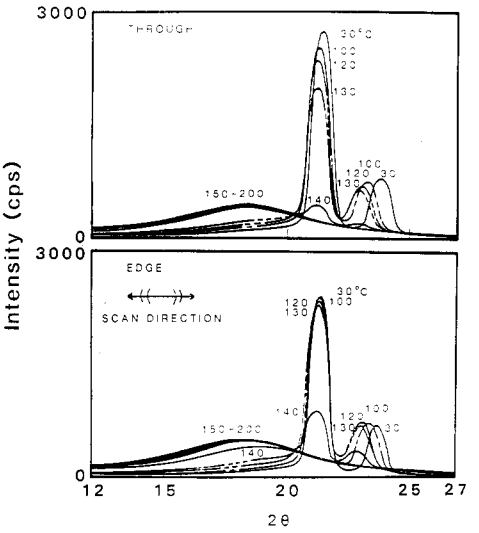

Figure 10. Variations of (110), (200), and amorphous scattering peaks as a function of temperature (a) in the through view and (b) in the equatorial direction of the edge view.

scans have been acquired in both equatorial and meridinal directions and are shown in Figure 11a on a comparable scale. As expected, the reduction of the (110) and (200) intensity with increasing temperature can be discerned in the meridinal direction as well. It is also noticed that the amorphous WAXD intensity has increased appreciably with annealing in the temperature range (100–140 °C), whereas the SAXS long period increases. It can be seen more clearly in Figure 12 that the apparent (directional dependent) crystallinity as estimated from the WAXD data of the through as well as of the edge view decreases with annealing temperature. Concurrently, the position of the (200) peak moves to lower Bragg's angles much more rapidly than that of the (110) plane in both through and edge views due to thermal expansion of the crystal a-axis accompanying the crystal transformation from orthorhombic to hexagonal structure. This is consistent with the earlier works by others.[8,10]

Above the crystal melting temperature, the (110) and (200) reflections disappear completely, suggesting that there are no superheated crystals in the present gelation crystallized UHMWPE. The amorphous WAXD peak in the through view does not show any appreciable changes in the melt state. However, the amorphous scattering in the equatorial region of the edge view increases slightly with continued heating while that in the polar region decreases in the melt state. This tendency is more prominent in the case of $M_w = 2 \times 10^6$ UHMWPE (Figure 11b). The decrease in the x-ray intensity may be attributed to the reduction of electron density of polyethylene melts with increasing temperature. In the equatorial region, this decrease is counterbalanced by an increase in the amount of amorphous chains due to the molecular diffusion of slowly melting UHMWPE crystals. It seems that amorphous chains are by no means random in the melt, retaining some preferential orientation in the thickness direction. Moreover, the amorphous scattering peak moves to low angles in both meridinal and equatorial directions, associated with an increase in the correlation distance (radial distribution function) of the amorphous materials.

The heterogeneity of UHMWPE melt was further investigated by using small angle light scattering. Figure 13 exhibits the V_v scattering patterns at temperatures below and above the crystal melting temperature. There are no appreciable changes in the scattering pattern. No H_v scattering was observed above the T_m. The lack of H_v

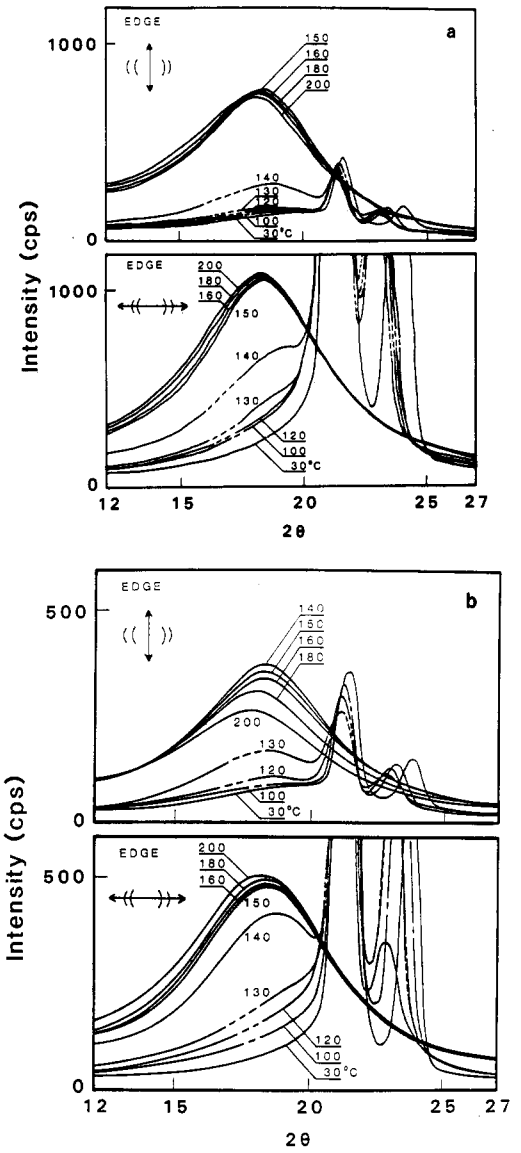

Figure 11. Variations of (110), (200), and amorphous scattering peaks as a function of temperature in the meridinal direction and in the equatorial direction of the edge view for the (a) $M_w = 6 \times 10^6$ and (b) $M_w = 2 \times 10^6$ UHMWPE.

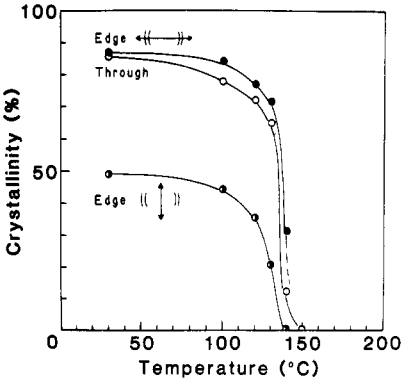

Figure 12. Variation of the directional dependent crystallinity of gelation crystallized UHMWPE as a function of annealing temperature.

scattering in the UHMWPE melt does not necessarily mean the absence of orientation fluctuations. It is quite possible that the fluctuation size may be too small such that it is not accessible with the wavelength of light. Another naive account is that all molecules are preferentially aligned normal to the film thickness, i.e., parallel to

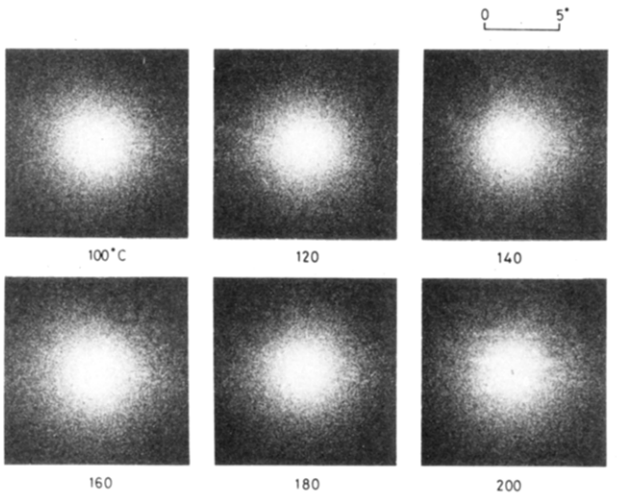

Figure 13. Change of V_v light scattering patterns during the course of heating. The incident light is normal to the film surface of the gelation crystallized UHMWPE.

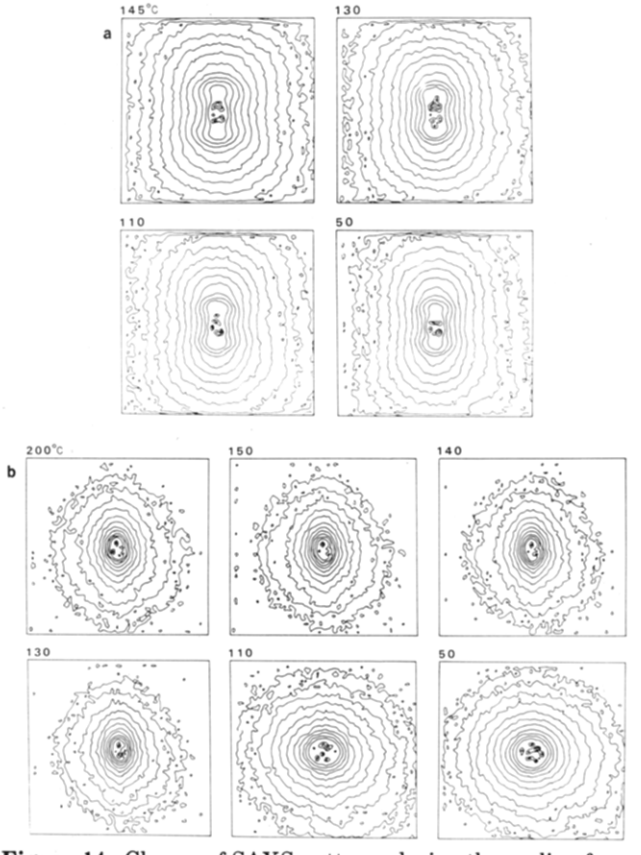

Figure 14. Change of SAXS patterns during the cooling from (a) 145 °C and (b) 200 °C.

the wave propagation direction; therefore, no polarization occurs. It is well-known that the scattering of light by liquid crystals is associated with the long-range orientation fluctuations and the relation of $I_{V_v} = (4/3)I_{H_v}$ generally holds.[17,18] The lack of H_v scattering suggests that there is no long-range order in the materials; thus the smectic or nematic liquid crystalline structure may not be present in the UHMWPE melts.

As can be seen in parts a and b of Figure 14, there is an appreciable difference in the formation of SAXS pattern during cooling from the melt of 145 and 200 °C. In the former case, the anisotropic SAXS pattern remains unchanged during crystallization, whereas in the latter, the pattern changes from anisotropic to isotropic structure at

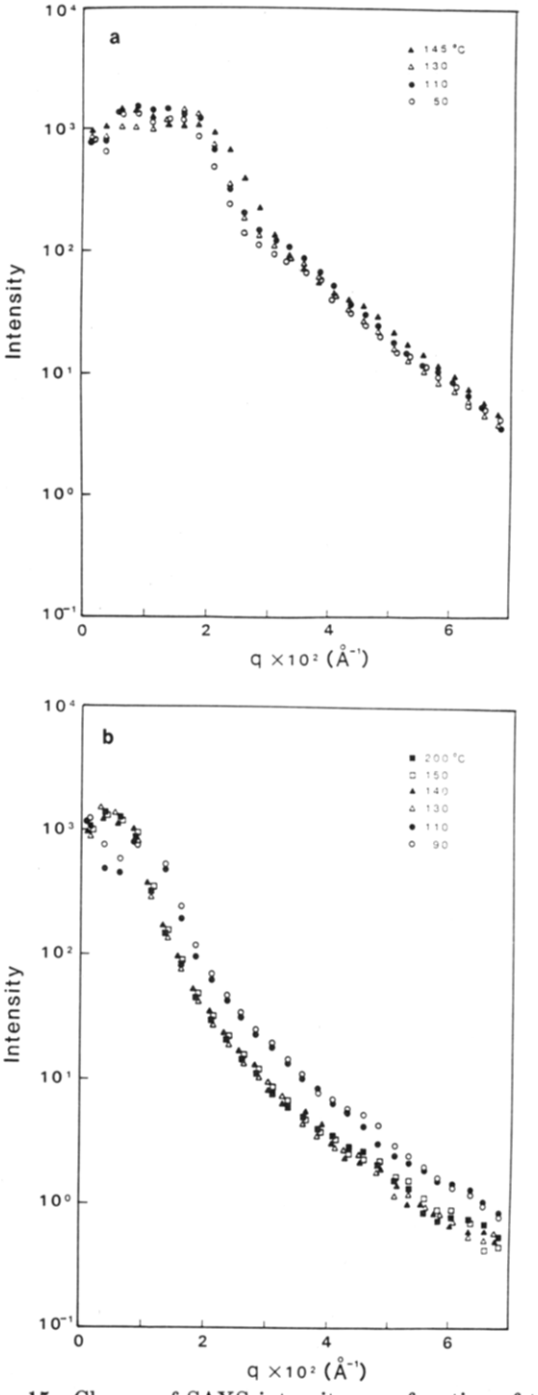

Figure 15. Change of SAXS intensity as a function of temperature after cooling from the melt: (a) 145 °C and (b) 200 °C.

the crystallization temperature. As can be noticed from Figure 15b, the SAXS curves in the edge view show no clear maximum and the intensity increases only slightly during the crystallization from the melt (200 °C). The SAXS intensity does not change either in magnitude or in shape when crystallized from 145 °C (Figure 15a). No superstructure was observed in the recrystallized specimen under light scattering or optical microscopic examinations. In the latter case, a well-grown truncated spherulite structure with well-defined concentric fringes was seen under the microscope as shown in Figure 16. The spherulitic size ranges from 20 to 200 μm in diameter. The average diameter of the spherulites is about 100 μm, and the periodicity of dark fringes is a few micrometers. In Figure 17 are shown the typical H_v, V_v, and H_h scattering patterns with arcs at a wider angle, characteristic of the lamellar twist period.

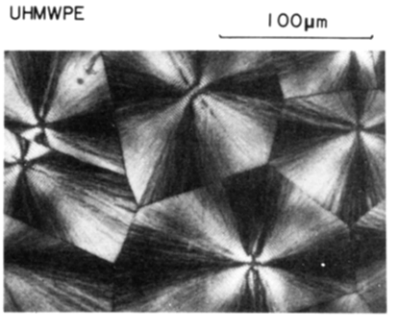

Figure 16. Development of banded spherulite structures in the gelation crystallized UHMWPE after recrystallization from the melt (200 °C).

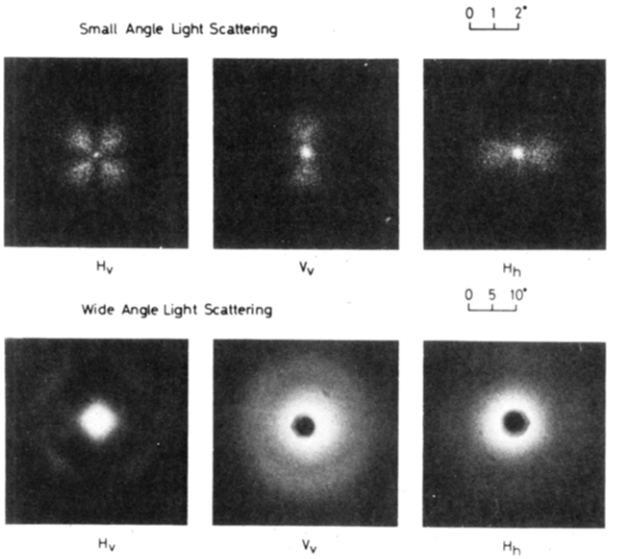

Figure 17. Small- and wide-angle light scattering patterns of melt crystallized UHMWPE gel films in the H_v, V_v, and H_h polarization configurations.

Discussion

First, we shall discuss the annealing below the crystal melting temperature. The increase of long period from 120 to 300 Å in the gelation crystallized UHMWPE is in agreement with the studies of single crystal mats by others.[15,19-21] This has been customarily interpreted in terms of a lamellar thickening process.[22,23] Recently, Kawaguchi and co-workers[19] found that the (110) reflection first decreased for about 30 s and then increased while the SAXS long period increased during the isothermal annealing studies on the polyethylene single crystal mats. The initial decrease of the WAXD (110) reflection has been attributed to the rapid reorganization of stacked lamellae associated with the partial melting or melting and recrystallization.[24,25] The subsequent increase has been explained as a result of increasing evenness of lamellar thickness. Grubb and co-workers[20,21] recently observed in the time-dependent synchrotron radiation studies of linear polyethylene single crystal mats ($M_w \sim 78000$) that the WAXD crystallinity initially decreased for some periods (2–4 s) then again increased with time. Meanwhile, the SAXS long period continuously increases. This observation has been attributed to the melting and recrystallization.

In the present case, the decrease of (110) and (200) planes and the increase of amorphous scattering with annealing temperature were observed in the through view as well as in both meridinal and equatorial scans of the edge view. The reduction of the directional dependent apparent crystallinity (Figure 12) strongly suggests that the increase in the long period cannot be explained simply in terms of lamellar thickening[22,23] in this gelation crystallized UHMWPE. We postulate that it may be associated with the partial melting of certain lamellae, thus giving rise to an increase in the periodic distance between lamellar structures. Because of the extremely high molecular weight of the material, the phenomenon of melting and recrystallization occurs rather slowly in the present case as compared with the conventional single crystal mats of Grubb et al.[20,21] where the process is completed within 4 s. Although our current SAXS apparatus is not capable of following the fast processes occuring within 2–30 s, as demonstrated by the previous authors,[19,20] time-dependent SAXS studies on this UHMWPE may still be feasible with the present setup. However, time-resolved WAXD experiment is not possible at this moment. Since the present study is not an isothermal experiment, the direct comparison with the results of Kawaguchi et al.[19] or Grubb et al.[21] is not warranted pending the completion of the said kinetic studies.[27]

One of the unique features in this study is the persistence of the SAXS and SALS scattering in the UHMWPE melt in the temperature range of 145–200 °C. The SAXS scattering occurs due to density fluctuations whereas the V_v light scattering arises from orientation, concentration, and density fluctuations. The WAXD studies show the presence of weakly anisotropic melts, which suggests that the UHWMPE melt is by no means homogeneous. This melt anisotropy, as pointed out by Zachariades and Logan[12] as well as Wunder and Merajver,[13] may be associated with the slow diffusion of the UHMWPE chains during melting. The oriented melt seems to be responsible for the appearance of the elliptical SAXS contour. This short-range orientation fluctuation gives rise to the V_v light scattering in the melt state. The lack of H_v scattering suggests that there are no long-range orientation fluctuations. Hence, it may be concluded that the smectic liquid crystalline structure is not present in the UHMWPE melt. The absence of smectic structure was also pointed out by Wunder and Merajver[13] from the Raman spectroscopic studies.

Another interesting observation in this study is the formation of well-grown truncated spherulites with well-defined lamellar twist periodicity. Since the melt viscosity of UHMWPE is extremely high, the molecular diffusion is expected to be slow. Hence, it is generally believed that the development of large spherulitic superstructures during the crystallization from the melt is highly unlikely. Recently, Zachariades[12] observed the development of large spherulites (approximately 250 μm in diameter) in the gel state. In the present melt recrystallized UHMWPE, the average diameter of the spherulites is about 100 μm; and, of course, the size can be over 200 μm in some locations. It should be pointed out that such spherulites developed only when the samples crystallized from high melt temperatures in excess of 200 °C. The cooling from 145 °C, which is slightly above the T_m, shows no spherulite development. The memory effect,[26] due to the slow diffusion of the melt, might influence the crystallization behavior of the gelation crystallized UHMWPE. The reason for the formation of such large spherulites is presently unclear, but we postulate that the lesser incorporation of chain entanglements in the gel structure may play an important role in the crystallization process. Even for conventional polyethylenes, it is unusual to obtain large spherulites of this order. There were only a few instances in the literature[28,29] that 100 μm size (diameter) spherulites were obtained in the specially prepared linear polyethylene virtually free from nucleating agent. Very recently, Rego

Lopez and Gedde[29] observed the development of very large spherulites (over 100 μm in diameter) in binary blends of linear polyethylenes. At present, the study on the crystallization kinetics of this gelation crystallized UHMWPE is in progress and will be reported in a future publication.[27]

Conclusions

We observed the melting and recrystallization during annealing at various temperatures near the T_m of gelation crystallized UHMWPE. The increase of SAXS long period in the present study may be due to an increase in the periodic distance of lamellar structure associated with the partial melting of certain lamellae rather than the lamellar thickening. The UHMWPE melt appears heterogeneous and anisotropic which may be a consequence of the slow diffusivity of UHMWPE chains during melting. The anisotropic melt gives rise to the small-angle scattering of X-ray and V_v light scattering. The smectic liquid crystalline structure may not be present in the UHMWPE. Large spherulites with distinct concentric fringes formed during crystallization from the melt (200 °C), but no superstructure developed during cooling from 145 °C.

Acknowledgment. The support of this work by the National Science Foundation, Grants MSM-8519906 and MSW-8713531 to the University of Akron, is gratefully acknowledged. This research is also sponsored in part by the National Science Foundation under Interagency Agreement DMR-8311769 and the U.S. Department of Energy under Contract DE-AC05-84OR21400 with Martin Marietta Energy Systems, Inc.

Registry No. PE, 9002-88-4.

References and Notes

(1) Zwijnenburg, A.; Pennings, A. J. *Colloid Polym. Sci.* **1976**, *254*, 868.
(2) Pennings, A. J.; Torfs, J. C. *Colloid Polym. Sci.* **1979**, *257*, 547.
(3) Smith, P.; Lemstra, P. J.; Kalb, B.; Pennings, A. J. *Polym. Bull. (Berlin)* **1979**, *1*, 733.
(4) Smith, P.; Lemstra, J. *Mater. Sci.* **1980**, *15*, 505.
(5) Smith, P.; Lemstra, P. J.; Booij, H. C. *J. Polym. Sci., Polym. Phys. Ed.* **1981**, *19*, 877.
(6) Smook, J.; Torfs, J. C.; van Hulten, P. F.; Pennings, A. J. *Polym. Bull. (Berlin)* **1980**, *2*, 293.
(7) Matsuo, M.; Manley, R. St. J. *Macromolecules* **1982**, *15*, 985.
(8) Pennings, A. J.; van der Mark, J. M.; Kiel, A. M. *Kolloid Z. Z. Polym.* **1970**, *237*, 334.
(9) deBoer, J.; van den Berg; Pennings, A. J. *Polymer* **1984**, *25*, 513.
(10) Matsuo, M.; Sawatari, C. *Macromolecules* **1986**, *19*, 2028.
(11) Zachariades, A. E.; Logan, J. A. *J. Polym. Sci., Polym. Phys. Ed.* **1983**, *21*, 821.
(12) Zachariades, A. E. *J. Appl. Polym. Sci.* **1986**, *32*, 4277.
(13) Wunder, S. L.; Merajver, S. D. *J. Polym. Sci., Polym. Phys. Ed.* **1986**, *24*, 99.
(14) Wunderlich, B. *Macromolecular Physics*; Academic Press: New York, 1973.
(15) Geil, P. H. *Polymer Single Crystals*; Wiley: New York, 1963.
(16) Schultz, J. M. *Polymer Materials Science*; Prentice-Hall: Englewood Cliffs, NJ, 1974.
(17) Chandrasekhar, S. *Liquid Crystals*; Cambridge University Press: Cambridge, 1977.
(18) Stein, R. S.; Rhodes, M. B. *J. Polym. Sci., Polym. Phys. Ed.* **1969**, *7*, 1539.
(19) Kawaguchi, A.; Ichida, T.; Murakami, S.; Katayama, K. *Colloid Polym. Sci.* **1984**, *262*, 597.
(20) Grubb, D. T.; Liu, J. H.; Caffrey, M.; Bilderback, D. H. *J. Polym. Sci., Polym. Phys. Ed.* **1984**, *22*, 367.
(21) Grubb, D. T.; Liu, J. H. *J. Appl. Phys.* **1985**, *58*, 2822.
(22) Fischer, E. W.; Schmidt, G. F. *Angew. Chem.* **1962**.
(23) Fischer, E. W. *Pure Appl. Chem.* **1972**, *31*, 113.
(24) Mandelkern, L.; Allou, A. L., Jr. *J. Polym. Sci., Polym. Lett. Ed.* **1966**, *4*, 447.
(25) Mandelkern, L.; Sharma, R. K.; Jackson, J. F. *Macromolecules* **1969**, *2*, 644.
(26) Chivers, R. A.; Barham, P. J.; Martinez-Salazar, J.; Keller, A. *J. Polym. Sci., Polym. Phys. Ed.* **1982**, *20*, 1717.
(27) Kyu, T.; Cho, M. H., to be submitted for publication.
(28) Hay, I. L.; Keller, A. *Kolloid Z. Z. Polym.* **1969**, *204*, 43.
(29) Rego Lopez, J. M.; Gedde, U. W. *Polymer* **1988**, *29*, 1037.

Structural Studies of Conducting Polymer Solutions and Films: Poly(3-methylthiophene)

D. Phil Murray,† Lowell D. Kispert,* and Steve Petrovic

Chemistry Department, The University of Alabama, Tuscaloosa, Alabama 35487

Jane E. Frommer

IBM Research Division, Almaden Research Center, 650 Harry Rd., San Jose, California 95120. *Received July 20, 1988; Revised Manuscript Received October 14, 1988*

ABSTRACT: 3-Methylthiophene has been polymerized by AsF_5 in AsF_3 solution to illustrate the complexity of the chemical and physical interactions which govern conducting polymer solubility and final film properties. The conducting polymer solutions and the electrically conductive films cast from them have been analyzed via solution- and solid-state NMR and EPR and SEM/EDX techniques. The AsF_6^- ion that has long been proposed as a dopant counterion has been identified at low dopant levels. Sulfur-centered radicals are observed in solution, and carbon-centered radicals are observed in the corresponding cast films. These carbon-based radicals appear to be uncorrelatable with the conductivity of the cast films. From SEM measurements, the electrical and mechanical properties of the electrically conductive poly(3-methylthiophene) films cast from solution are found to be dependent on the sample morphology.

I. Introduction

Electrically conductive polymers are polymers with highly conjugated π-electron systems which although insulating in their pristine state exhibit an extremely large increase in their electrical conductivity upon chemical or electrochemical oxidation or reduction (a process referred to as "doping"). For example, the conductivity of poly(*p*-phenylene sulfide) (PPS) increases 10^{16} upon oxidative doping with AsF_5. These materials combine the properties of plastics and metals making them potentially applicable to lightweight energy storage devices and electronic circuitry devices.[1,2] However, most conducting polymers

† Present address: Dow Chemical, USA, M. E. Pruitt Research Center, Midland, MI 48674.

0024-9297/89/2222-2244$01.50/0